

Singular ferromagnetic susceptibility of the transverse-field Ising antiferromagnet on the triangular lattice

Sounak Biswas¹ and Kedar Damle¹

¹Tata Institute of Fundamental Research, 1 Homi Bhabha Road, Mumbai 400005, India

A transverse magnetic field Γ is known to induce antiferromagnetic three-sublattice order of the Ising spins σ^z in the triangular lattice Ising antiferromagnet at low enough temperature. This low-temperature order is known to melt on heating in a two-step manner, with a power-law ordered intermediate temperature phase characterized by power-law correlations at the three-sublattice wavevector \mathbf{Q} : $\langle \sigma^z(\vec{R}) \sigma^z(0) \rangle \sim \cos(\mathbf{Q} \cdot \vec{R}) / |\vec{R}|^{\eta(T)}$ with the temperature-dependent power-law exponent $\eta(T) \in (1/9, 1/4)$. Here, we use a newly developed quantum cluster algorithm to study the *ferromagnetic* easy-axis susceptibility $\chi_u(L)$ of an $L \times L$ sample in this power-law ordered phase. Our numerical results are consistent with a recent prediction of a singular L dependence $\chi_u(L) \sim L^{2-9\eta}$ when $\eta(T)$ is in the range $(1/9, 2/9)$. This finite-size result implies, via standard scaling arguments, that the ferromagnetic susceptibility $\chi_u(B)$ to a uniform field B along the easy axis is singular at intermediate temperatures in the small B limit, $\chi_u(B) \sim |B|^{-\frac{4-18\eta}{4-9\eta}}$ for $\eta(T) \in (1/9, 2/9)$, although there is no ferromagnetic long-range order in the low temperature state.

PACS numbers: 75.10.Jm

I. INTRODUCTION

The transverse field Ising antiferromagnet on the triangular lattice, with Hamiltonian,

$$H_{\text{Ising}} = J_1 \sum_{\langle \vec{R}\vec{R}' \rangle} \sigma_{\vec{R}}^z \sigma_{\vec{R}'}^z - \Gamma \sum_{\vec{R}} \sigma_{\vec{R}}^x - B \sum_{\vec{R}} \sigma_{\vec{R}}^z, \quad (1)$$

where $\vec{\sigma}_{\vec{R}}$ are Pauli matrices representing $S = 1/2$ moments on sites \vec{R} of the triangular lattice, $\langle \vec{R}\vec{R}' \rangle$ denote the nearest neighbour links of the triangular lattice, $J_1 > 0$ is the antiferromagnetic exchange among easy-axis components of the $S = 1/2$ moments (a factor of $\frac{1}{4}$, appropriate for $S = 1/2$ moments, has been absorbed in the definition of J_1), and B and Γ are components of the external magnetic field along the easy axis \hat{z} and transverse direction \hat{x} respectively (a factor of $\frac{g\mu_B}{2}$, appropriate for $S = 1/2$ moments, has been absorbed in the definition of these field components), provides perhaps the simplest example of a quantum “order-by-disorder”^{1,2} effect, whereby a classical spin liquid develops long-range magnetic order upon the introduction of terms in the Hamiltonian that induce quantum fluctuations.

When $\Gamma = 0$, the zero temperature classical Ising antiferromagnet at $B = 0$ has a macroscopic degeneracy of minimum exchange-energy configurations on the triangular lattice. These are in correspondence with all dimer covers of the dual honeycomb lattice, implying that the entropy-density remains nonzero in this classical zero temperature limit.^{3,4} At non-zero temperature, thermal fluctuations of σ^z allow for defects that take the system out of the minimum exchange-energy dimer subspace. The Ising spins remain in a paramagnetic state all the way down to $T = 0$,^{3,4} albeit with a diverging correlation length⁵ at the three-sublattice wavevector \mathbf{Q} . This provides a simple example of classical spin liquid behaviour, with the $T = 0$ limit characterized by power-

law spin correlations at the three-sublattice wavevector \mathbf{Q} .

A transverse field Γ that couples to σ^x induces quantum fluctuations of the Ising spins σ^z , and would ordinarily be expected to further reduce any residual ordering tendency of the Ising spins. However, in reality, these quantum fluctuations immediately stabilize a ground-state with long-range three-sublattice order of σ^z for any nonzero Γ . In contrast to the *ferrimagnetic* three-sublattice order exhibited by the classical Ising antiferromagnet with ferromagnetic further neighbour couplings⁶, the $\Gamma > 0$ ground state is characterized by *antiferromagnetic* three-sublattice order,⁷ i.e., the modulation of $\langle \sigma^z \rangle$ at wavevector \mathbf{Q} is not accompanied by any net ferromagnetic moment. At $T = 0$, this three-sublattice order persists up to a critical value $\Gamma_c \approx 1.7^7$ (in units of J_1), beyond which the system becomes a quantum paramagnet in which the spins are polarized in the \hat{x} direction.^{2,7,8} When the system is heated to nonzero temperatures above this three-sublattice ordered ground state, the three-sublattice order melts via an intermediate-temperature phase characterized by power-law order: $\langle \sigma^z(\vec{R}) \sigma^z(0) \rangle \sim \cos(\mathbf{Q} \cdot \vec{R}) / |\vec{R}|^{\eta(T)}$ for $T \in (T_1, T_2)$, with a temperature-dependent power-law exponent $\eta(T)$ that is expected⁹ to increase from $\eta(T_1) = 1/9$ to $\eta(T_2) = 1/4$.⁷

A recent field-theoretical analysis¹⁰ predicts that the *ferromagnetic easy-axis susceptibility* $\chi_u(B)$ to the uniform longitudinal field B along the easy-axis diverges at small B in a large portion of such power-law ordered phases associated with the two-step melting of three-sublattice order in frustrated easy-axis antiferromagnets with triangular lattice symmetry: $\chi_u(B) \sim |B|^{-\frac{4-18\eta}{4-9\eta}}$ for $\eta(T) \in (1/9, 2/9)$. For the specific case of the transverse field Ising antiferromagnet on the triangular lattice, this is a rather counter-intuitive prediction: The Ising spins in Eq. (1) have no ferromagnetic couplings, and

ferromagnetic correlations remain short-ranged in the low-temperature phase with long-range three-sublattice ordered phase. Yet, the prediction is for the uniform easy-axis susceptibility to start diverging once this three-sublattice order melts partially due to thermal fluctuations.

Our goal here is to test this general prediction using the test-bed provided by the transverse field Ising antiferromagnet (Eq. (1)) on the triangular lattice. In order to do this, we need to obtain an accurate characterization of the long-distance form of the correlations of the easy-axis magnetization density as well as correlations of the three-sublattice order parameter for this model. These can be used to obtain the finite-size easy-axis susceptibility $\chi_u(L)$ of the Ising spins, as well as the value of $\eta(T)$ for a range of temperatures in the power-law ordered phase. If the easy-axis susceptibility is indeed singular as predicted, then standard finite-size scaling arguments imply that $\chi_u(L) \sim L^{2-9\eta}$ for $\eta(T) \in (1/9, 2/9)$ in the power-law ordered phase. In this paper, we test this form of the prediction using a newly developed quantum-cluster algorithm¹¹ that provides an efficient tool for performing Quantum Monte Carlo simulations of frustrated transverse field Ising models within the Stochastic Series Expansion^{12,13} framework.

The rest of this paper is organized as follows: In Section. II, we discuss the antiferromagnetic nature of the three-sublattice order induced by the transverse field and contrast it with the ferrimagnetic three-sublattice ordered phase established by additional ferromagnetic couplings. We also review the standard Landau theory framework used for describing this kind of long-range order, and use it to discuss the possible theoretical scenarios for the phase transition between these two phases. In Section. III we provide a brief sketch of the actual computational method used to obtain our numerical results. In Section. IV, we summarize our results for the uniform magnetization density as well as the three-sublattice order parameter and compare them with the field-theoretical predictions alluded to earlier.

II. PHASES AND TRANSITIONS

The *antiferromagnetic* (with no net easy-axis magnetic moment) three-sublattice order exhibited by the $\Gamma > 0$ ground state of H_{Ising} can be thought of in terms of the following useful caricature: Ising spins on one spontaneously chosen sublattice (out of the three sublattices corresponding to the natural tripartite decomposition of the triangular lattice) freeze into the $|\sigma^x = +1\rangle$ state. Equivalently, one may think of them as fluctuating freely between the $|\sigma^z = +1\rangle$ and $|\sigma^x = -1\rangle$ states due to the effects of quantum fluctuations. On the other two sublattices of the triangular lattice, the system orders antiferromagnetically, with spins on one sublattice pointing up along the \hat{z} axis, and spins on the other sublattice pointing down. This is also the picture for the long-

range ordered phase that persists up to the lower-critical temperature $T_1(\Gamma)$ that marks the onset of the power-law ordered intermediate phase associated with the two-step melting of three-sublattice order.

On incorporating an additional next-neighbour ferromagnetic coupling $J_2 < 0$, the antiferromagnetic three-sublattice order of the low-temperature phase gives way to *ferrimagnetic* (with net easy axis moment) three-sublattice order beyond a non-zero threshold value J_{2c} .¹¹ This is because the classical ($\Gamma = 0$) model with $J_2 < 0$ is known to develop ferrimagnetic three-sublattice order beyond a $T = 0$ threshold at which σ^z have power-law correlators $\langle \sigma^z(\vec{R})\sigma^z(0) \rangle \sim \cos(\mathbf{Q} \cdot \vec{R})/|R|^\eta$ with $\eta = 1/9$.¹⁴ This ferrimagnetic three-sublattice order can be understood in terms of the following caricature: The system spontaneously chooses one sublattice on which the spins all point along the $+\hat{z}$ direction ($-\hat{z}$ direction), while the spins on the other two sublattices all point along the $-\hat{z}$ direction ($+\hat{z}$ direction).

With this picture of the low temperature phases in mind, we focus our attention on the uniform easy axis magnetization m and the complex three-sublattice order parameter ψ , defined as

$$m = \frac{1}{L^2} \sum_{\vec{R}} \sigma_{\vec{R}}^z \quad (2)$$

$$\psi = \frac{1}{L^2} \sum_{\vec{R}} \sigma_{\vec{R}}^z \exp(i\mathbf{Q} \cdot \vec{R}) \quad (3)$$

where \mathbf{Q} is the three-sublattice ordering wave vector ($(2\pi/3, 2\pi/3)$ in the standard basis) and \vec{R} represents the coordinates of triangular lattice sites. In the standard Landau-Ginzburg approach¹⁵⁻¹⁷ to thermal (nonzero temperature) phase transitions involving such three-sublattice ordered states, the physics of three-sublattice ordering is represented in terms of a classical order parameter field ψ_{cl} , which may be identified with the static (Matsubara frequency $\omega_n = 0$) part of the ψ operator defined above:

$$\psi_{\text{cl}} = \frac{1}{\beta} \int_0^\beta d\tau \psi(\tau) \quad (4)$$

Here, we used the usual notation for the imaginary-time analog of Heisenberg operators, $\mathcal{O}(\tau) = e^{\tau H_{\text{TFIM}}} \mathcal{O} e^{-\tau H_{\text{TFIM}}}$, corresponding to any Schrödinger operator \mathcal{O} .

In this Landau-Ginzburg framework, the free energy is written as an integral over a coarse-grained free-energy density $\mathcal{F}(\psi_{\text{cl}})$ that admits an expansion in powers and gradients of a coarse-grained order-parameter field $\psi_{\text{cl}}(\vec{r})$ which may be thought of as a local version of the order parameter defined in Eq. 4. Keeping various low-order terms consistent with the action of various symmetries

of the microscopic Hamiltonian, one writes:

$$\begin{aligned}\mathcal{F}(\psi_{\text{cl}}) = & \kappa|\nabla\psi_{\text{cl}}|^2 + r|\psi_{\text{cl}}|^2 + u_4|\psi_{\text{cl}}|^4 \\ & + u_6|\psi_{\text{cl}}|^6 + \lambda_6|\psi_{\text{cl}}|^6 \cos(6\theta) \\ & + \lambda_{12}|\psi_{\text{cl}}|^{12} \cos(12\theta) + \dots\end{aligned}\quad (5)$$

where, $\theta(\vec{r})$ is the phase of the complex order parameter field $\psi_{\text{cl}}(\vec{r})$. As usual, one assumes that the coefficients of various terms in this phenomenological free-energy are smooth functions of microscopic parameters. In this approach, three-sublattice ordering corresponds to $r < 0$. The sign of λ_6 determines the nature of three-sublattice ordering: $\lambda_6 > 0$ favors antiferromagnetic ordering with the phase θ pinned at $(2n+1)\pi/6$ ($n = 0, 1 \dots 5$), while $\lambda_6 < 0$ favors ferrimagnetic ordering with the phase pinned at $(2n)\pi/6$ ($n = 0, 1 \dots 5$). The λ_{12} term is not expected to be important except when λ_6 is driven to the vicinity of zero by the competition between further-neighbour ferromagnetic couplings (in the microscopic Hamiltonian) that favour ferrimagnetic three-sublattice ordering, and other effects (such as quantum fluctuations induced by a transverse field) that favour antiferromagnetic three-sublattice ordering.

If fluctuations of θ , the phase of the order parameter, play a dominant role in driving the transition to a paramagnetic high-temperature state, one expects a phase-only description to capture the long-wavelength properties near such a transition. In other words, one then expects that $|\psi_{\text{cl}}|$, the amplitude of the order parameter, remains nonzero near the transition (corresponding to $r < 0$), and the physics of the transition is controlled by the interplay between the effective phase-stiffness $\kappa|\psi_{\text{cl}}|^2$ and the six-fold anisotropy λ_6 . This gives rise to the expectation^{15–17} of critical behaviour in the universality class of the six-state clock model^{9,18,19} of statistical mechanics.

As is well-known, two-dimensional six-state clock models represent an unusual example of a system which can display a variety of critical behaviours, each of which is a generic possibility that can be realized for a range of microscopic parameters.¹⁹ Of particular interest in the present context is the possibility of a two-step melting transition, whereby the low-temperature phase with long-range order in $\exp(i\theta)$ is separated from a high-temperature paramagnetic phase by an intermediate phase with power-law order in $\exp(i\theta)$. As is well known, this power-law ordered phase is controlled by a line of Gaussian fixed points⁹ with effective free-energy density $\frac{1}{4\pi g} \int d^2r (\nabla\theta)^2$. For $g \in (1/9, 1/4)$, the six-fold anisotropy λ_6 and the vorticity in the xy field θ are both irrelevant perturbations of this fixed-point free-energy density, which controls the long-wavelength behaviour of order parameter correlations in the intermediate power-law ordered phase. The continuously varying power-law exponent $\eta(T)$ for order parameter correlations, which serves as a “universal coordinate” that locates a given microscopic system within this power-law ordered phase, is set by the coupling constant g via the

relation $\eta(T) = g(T)$.

The Landau-Ginzburg theory also sheds light on the nature of the low temperature transition between the two kinds of three-sublattice ordered phases, modeled by λ_6 going through zero smoothly and changing sign. Since both phases have long-range three-sublattice order, fluctuations of $|\psi_{\text{cl}}|$ may again be neglected in the vicinity of this transition. With the amplitude $|\psi_{\text{cl}}|$ remaining essentially constant across this transition, the physics of the transition is again controlled by the phase θ of the three-sublattice order parameter. Minimizing the free-energy density \mathcal{F} yields a spatially uniform configuration with a particular optimal value θ^* for this phase variable. When $\lambda_{12} < 0$, θ^* takes on the values $(2n+1)\pi/6$ ($(2n)\pi/6$) with $n = 0, 1 \dots 5$ when $\lambda_6 > 0$ ($\lambda_6 < 0$). When $\lambda_6 = 0$, all values $\theta^* = m\pi/6$ ($m = 0, 1 \dots 11$) minimize the free-energy. Clearly, this corresponds to a first-order transition between ferrimagnetic and antiferromagnetic three-sublattice ordered states, with both kinds of three-sublattice order coexisting at the transition point.

If, on the other hand, $\lambda_{12} > 0$, we obtain

$$\theta^* = \begin{cases} \frac{2n\pi}{6} & \text{if } \lambda_6 < -4\lambda_{12}|\psi_{\text{cl}}|^6 \\ \frac{2n\pi}{6} + \frac{1}{6} \arccos(-\lambda_6/4\lambda_{12}|\psi_{\text{cl}}|^6) & \text{if } |\lambda_6| < 4\lambda_{12}|\psi_{\text{cl}}|^6 \\ \frac{(2n+1)\pi}{6} & \text{if } \lambda_6 > 4\lambda_{12}|\psi_{\text{cl}}|^6 \end{cases} \quad (6)$$

where $n = 0, 1 \dots 5$ represents the six-fold degeneracy of the minima in each case. In this case, as $|\lambda_6|$ becomes small and λ_6 goes through zero, θ^* switches continuously from the antiferromagnetic phase to the ferrimagnetic phase via an intermediate mixed phase that is established for $|\lambda_6| < 4\lambda_{12}|\psi_{\text{cl}}|^6$. In what follows, we will confront these two quite different scenarios with data obtained in the vicinity of the transition between antiferromagnetic and ferrimagnetic three-sublattice order in the low-temperature state of H_{Ising} with an additional ferromagnetic second-neighbour coupling J_2 between the Ising spins.

III. METHODS

Our numerical work uses the Stochastic Series Expansion (SSE) framework^{12,13,20–22} to compute equilibrium averages $\langle \dots \rangle$ for transverse field Ising models at nonzero temperature. For models with geometric frustration, which results in a macroscopic degeneracy of minimally frustrated classical configurations (with minimum Ising-exchange energy), it is important that the computational method correctly captures the interplay between this macroscopic degeneracy, and the disordering effects of classical and quantum fluctuations. In the present case, this interplay is expected to be crucial to the establishment of antiferromagnetic three-sublattice order in the low temperature phase, as well as its two-step melting.^{2,7,8}

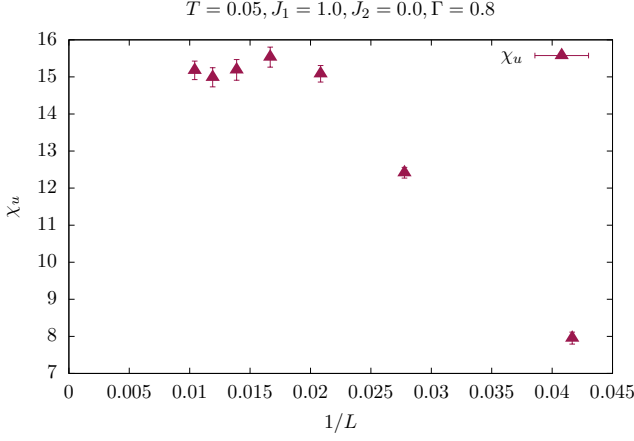


FIG. 1. The uniform easy-axis susceptibility χ_u of H_{Ising} on $L \times L$ triangular lattices, when plotted vs $1/L$ for a sequence of sizes, clearly saturates to a finite value in the limit of large L . Note the slow crossover to this thermodynamic limit, with samples of linear size as large as $L^* = 40$ not yet in the asymptotic large- L regime. This behaviour demonstrates that the low temperature phase is indeed antiferromagnetic. However, the slow crossover indicates the presence of a proximate phase with net magnetic moment along the easy-axis, suggesting that H_{Ising} could be driven into a ferrimagnetic ground state for relatively small values of an additional second-neighbour ferromagnetic coupling J_2 . All other temperature and energy scales are measured in units of J_1 which is set to unity.

Therefore, to obtain reliable results, we use the recently developed quantum cluster algorithm¹¹ that works within the SSE framework to provide an efficient way of sampling the partition function for such frustrated transverse field Ising models. In this cluster algorithm, which works in the σ^z basis, the diagonal Ising exchange part of H_{Ising} in Eq. (??) is written as $\mathcal{H}_{\text{diag}} = \sum_{\Delta} \mathcal{H}_{\Delta}$, where H_{Δ} are operators living on elementary triangular plaquettes Δ . This furnishes the algorithm local information that enables it to distinguish between minimally frustrated plaquettes and fully frustrated plaquettes of higher Ising-exchange energy. The transverse field part of the Hamiltonian is represented as single-site operators as in the original SSE approach.¹³ The plaquette representation of $\mathcal{H}_{\text{diag}}$ facilitates the construction of “space-time clusters” with a broad distribution of cluster sizes, allowing the algorithm to efficiently sample the configuration space of SSE operator strings at low temperature.

Using this approach, we study H_{Ising} on $L \times L$ triangular lattice with periodic boundary conditions, with L ranging from $L = 24$ to 96. We compute the static susceptibilities corresponding to the order parameters defined in Eq. (2). These susceptibilities are defined as

$$\chi_u = \frac{L^2}{\beta} \langle |\int_0^\beta d\tau m(\tau)|^2 \rangle \quad (7)$$

$$\chi_{\mathbf{Q}} = \frac{L^2}{\beta} \langle |\int_0^\beta d\tau \psi(\tau)|^2 \rangle \quad (8)$$

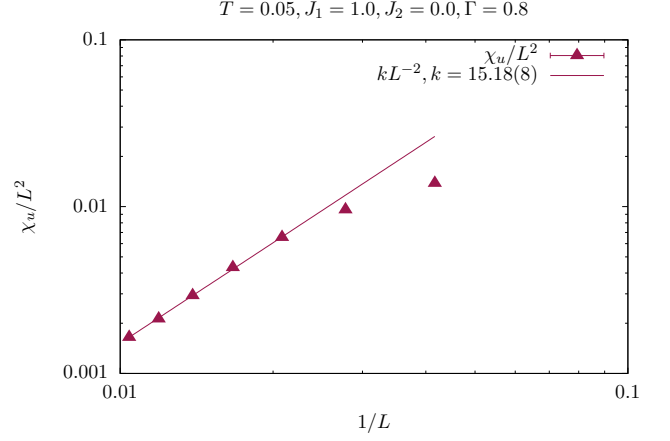


FIG. 2. The uniform easy-axis susceptibility of H_{Ising} on $L \times L$ triangular lattices, now scaled by the number of sites L^2 , is fit reasonably well to the single parameter form kL^{-2} with $k = 15.18(8)$ for the largest four sizes studied here. This analysis also confirms that the low temperature phase of H_{Ising} is indeed antiferromagnetic, *i.e.* with no net easy-axis moment. All other temperature and energy scales are measured in units of J_1 which is set to unity.

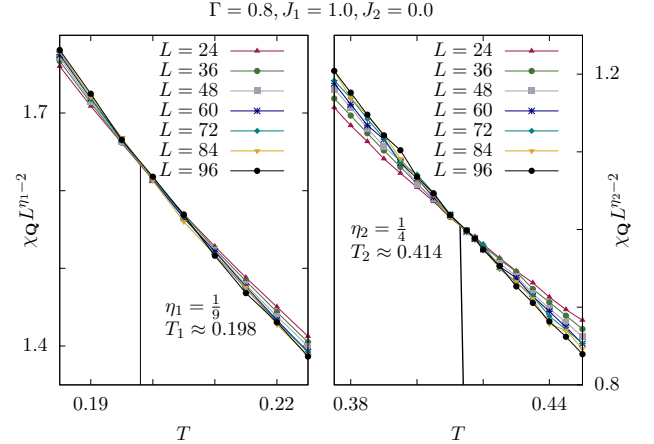


FIG. 3. Lower and upper transition temperatures T_1 and T_2 , which mark the boundaries of the power-law ordered phase associated with the two-step melting of antiferromagnetic three-sublattice order, are obtained by plotting $\chi_{\mathbf{Q}} L^{\frac{1}{9}-2}$ and $\chi_{\mathbf{Q}} L^{\frac{1}{4}-2}$ versus T for different values of L and identifying the temperatures at which curves corresponding to different L cross. This gives $T_1 = 0.198(5)$ and $T_2 = 0.414(5)$ when $\Gamma = 0.8$. All other temperature and energy scales are measured in units of J_1 which is set to unity.

Additionally, we compute the static susceptibility $\chi_{\mathbf{Q}}^{xx}$ to a transverse field (along \hat{x}) oscillating at wavevector \mathbf{Q} , defined as

$$\chi_{\mathbf{Q}}^{xx} = \frac{L^2}{\beta} \langle |\int_0^\beta d\tau \sigma_{\mathbf{Q}}^x(\tau)|^2 \rangle \quad (9)$$

where $\sigma_{\mathbf{Q}}^x$ is given by

$$\sigma_{\mathbf{Q}}^x = \frac{1}{L^2} \sum_{\vec{R}} \sigma_{\vec{R}}^x \exp(i\mathbf{Q} \cdot \vec{R}) \quad (10)$$

IV. RESULTS

We begin by revisiting the phase diagram obtained in previous work⁷ for the case with no next-nearest neighbour coupling ($J_2 = 0$). From their results, we note that the low temperature order persists up to the highest temperature when Γ is in the vicinity of $\Gamma = 0.8$. Therefore, we set the transverse field to this value in most of our work and study the three-sublattice ordering of the low temperature phase, as well as its two-step melting.

As expected, we find that the order parameter susceptibility $\chi_{\mathbf{Q}}$ scales with the volume of the system at low enough temperature, confirming the presence of long-range three-sublattice order in the low temperature phase. Since this is entirely consistent with earlier results,⁷ we do not display this explicitly here. Since our focus in what follows will be an unusual singular behaviour in the ferromagnetic susceptibility χ_u to a *uniform* field along the easy-axis, we find it useful to first study the same quantity deep in the low-temperature ordered state. From Fig. 1 and Fig. 2, which display the L dependence of χ_u and χ_u/L^2 deep in the low-temperature ordered state, we see that the three-sublattice ordering in the low temperature phase is not accompanied by any net moment along the easy-axis.

This confirms earlier results⁷ that have identified the antiferromagnetic nature of the three-sublattice ordering at low temperature. However, the approach to the thermodynamic limit is seen to involve a slow crossover, suggesting the presence of a proximate phase with a net easy-axis moment. This is consistent with the fact that a relatively small value of second-neighbour ferromagnetic exchange $J_2 < 0$ is sufficient to access a nearby state with ferrimagnetic three-sublattice ordering at low temperature.¹¹

In the power-law ordered phase associated with the two-step melting of three-sublattice order, the static susceptibility $\chi_{\mathbf{Q}}$, defined in Eq. (8) for a finite size $L \times L$ system, is expected to scale as

$$\chi_{\mathbf{Q}} \sim L^{2-\eta(T)} \quad (11)$$

From the renormalization group picture (summarized in the previous section) of this power-law ordered phase, it is also clear that $\eta(T)$ ranges from $\eta(T_1) = 1/9$ at the lower phase boundary $T_1(\Gamma)$ of the power-law phase, to $\eta(T_2) = 1/4$ at the upper phase boundary $T_2(\Gamma)$.

To locate these upper and lower transition temperatures for $\Gamma = 0.8$, we plot $\chi_{\mathbf{Q}} L^{\frac{1}{9}-2}$ and $\chi_{\mathbf{Q}} L^{\frac{1}{4}-2}$ for various sizes L as a function of temperature and identify the temperature at which curves corresponding to the different sizes all cross. This is shown in Fig. 3. The location

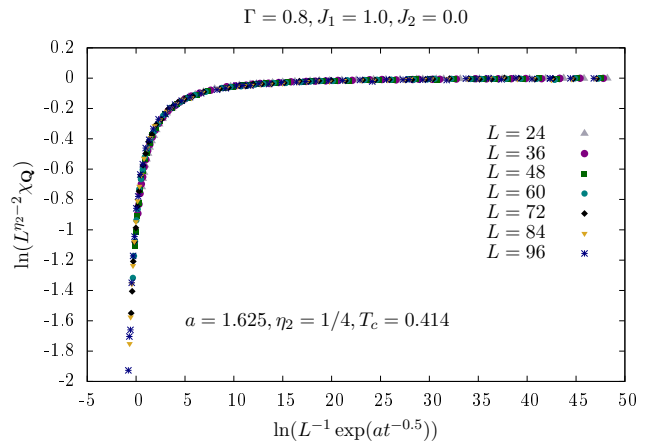


FIG. 4. Quantum Monte Carlo data for the static susceptibility $\chi_{\mathbf{Q}}$ of H_{Ising} at wavevector \mathbf{Q} on $L \times L$ triangular lattices collapses onto a universal scaling form when $\chi_{\mathbf{Q}}(t, L)L^{\frac{1}{4}-2}$ for different L and temperatures T (in the vicinity of the upper transition temperature T_2) are plotted as a function of the scaling variable defined in Eq. (13) in the main text. All other temperature and energy scales are measured in units of J_1 which is set to unity.

of transitions obtained in this way are consistent with those obtained earlier in Ref. 7.

Since the upper (lower) transitions out of the power-law ordered phase correspond to vorticity (six-fold anisotropy) in θ becoming relevant, we expect these transitions to be of the Kosterlitz-Thouless (inverted Kosterlitz-Thouless) type. To confirm that this is indeed the case, we perform fits of our Quantum Monte Carlo data in the vicinity of the upper phase boundary to the finite-size scaling form predicted by Kosterlitz-Thouless theory.¹⁸ This scaling form follows from the following argument: Above $T_2(\Gamma)$, order parameter correlations decay exponentially, with a correlation length ξ given by²³

$$\xi \sim \exp(at^{-1/2}), \quad (12)$$

where $t = (T - T_2)/T_2$ is the reduced temperature. This Kosterlitz-Thouless form of the correlation length, Eq. (12), in conjunction with the standard finite size scaling ansatz $\chi_{\mathbf{Q}}(t, L) = L^{2-\eta_2} f(\xi/L)$ gives the finite-size scaling form¹⁸

$$\chi_{\mathbf{Q}}(t, L)L^{\frac{1}{4}-2} = f(L^{-1} \exp(at^{-1/2})), \quad (13)$$

where we have used $\eta_2 = 1/4$, and f is the finite-size scaling function that we expect our data to collapse onto. In practice, we use T_2 obtained from Fig. 3, and attempt a finite-size scaling collapse with a single adjustable parameter a . This is shown in Fig. 4.

When ferromagnetic second-neighbour interactions $J_2 < 0$ of sufficient magnitude are present, one expects the ground state ordering pattern to change to ferrimagnetic three-sublattice order.¹⁴ In recent work,¹¹ the

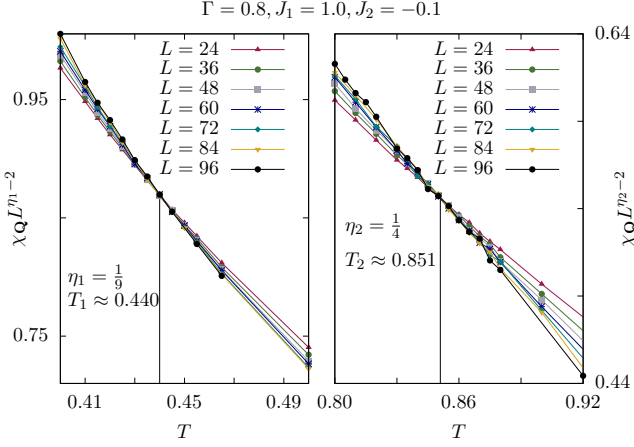


FIG. 5. The ferrimagnetic three-sublattice order that characterizes the ground state in the presence of a second-neighbour ferromagnetic interaction $J_2 = -0.1$ also melts in a two-step manner. Upper and lower transition temperatures T_1 and T_2 , that demarcate the boundaries of the power law ordered phase associated with this two-step melting, are obtained by plotting $\chi_Q L^{\frac{1}{9}-2}$ and $\chi_Q L^{\frac{1}{4}-2}$ versus T for different values of L and identifying the temperatures at which curves corresponding to different L cross. This gives $T_1 = 0.440(6)$ and $T_2 = 0.851(8)$ when $\Gamma = 0.8$. All other temperature and energy scales are measured in units of J_1 which is set to unity.

threshold value of J_2 corresponding to this onset of ferrimagnetism was estimated to be roughly $J_{2c} \approx -0.03$. With a view towards comparing the melting behaviour of this ferrimagnetic three-sublattice order with the two-step melting of antiferromagnetic three-sublattice order, we also study the effect of thermal fluctuations at $J_2 = -0.1$, *i.e.* deep in this ferrimagnetic three-sublattice ordered state. We find that long-range order is again lost via a two-step melting process, with an intermediate power-law ordered phase. The locations of the upper and lower transitions that demarcate the extent of the power-law ordered phase are obtained as before. This is displayed in Fig. 5. Above T_2 , the static order parameter susceptibility again collapses quite convincingly on to the Kosterlitz-Thouless finite-size scaling form. This is shown in Fig. 6.

With these preliminaries out of the way, we are now in a position to study in a unified way the behaviour of the uniform easy-axis susceptibility χ_u in the power-law ordered phase associated with the two-step melting of antiferromagnetic three-sublattice order as well as ferrimagnetic three-sublattice order. As mentioned earlier, our goal is to test a recent prediction¹⁰ that χ_u provides a thermodynamic signature of two step melting due to the presence of a singular B dependence: $\chi_u(B) \sim |B|^{-\frac{4-18\eta}{4-9\eta}}$ for $\eta(T) \in (1/9, 2/9)$.

Here, we test this via the equivalent prediction¹⁰ for the finite-size susceptibility $\chi_u(L)$ of an $L \times L$ sample when $B = 0$: $\chi_u(L) \sim L^{2-9\eta}$ for $\eta(T) \in (1/9, 2/9)$. In Landau theory terms, this singularity in χ_u is a direct

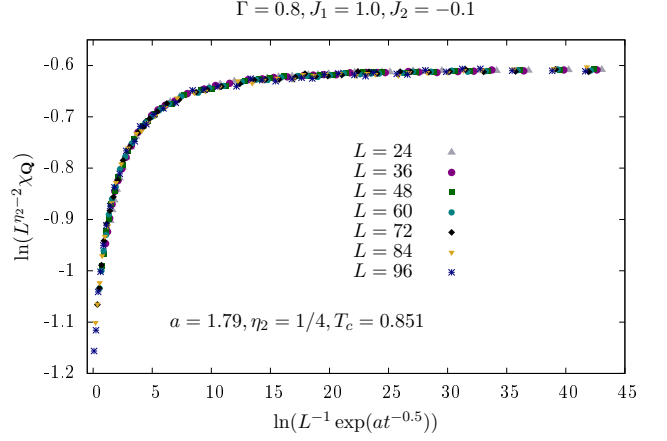


FIG. 6. Quantum Monte Carlo data for the static susceptibility χ_Q of H_{Ising} with $J_2 = -0.1$ at wavevector \mathbf{Q} on $L \times L$ triangular lattices also collapses onto a universal scaling form when $\chi_Q(t, L)L^{\frac{1}{4}-2}$ for different L and temperatures T (in the vicinity of the upper transition temperature T_2) are plotted as a function of the scaling variable defined in Eq. (13) in the main text. All other temperature and energy scales are measured in units of J_1 which is set to unity.

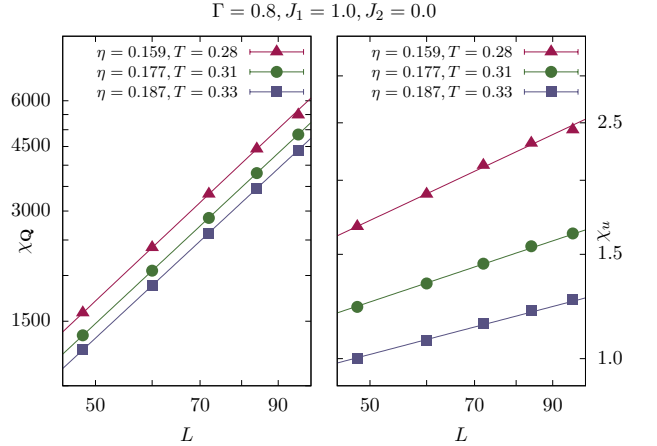


FIG. 7. χ_Q and χ_u fit rather well to power-law forms $k_1 L^{2-\eta}$ and $k_2 L^{2-9\eta}$ respectively for three different values of temperature in the intermediate power-law ordered phase associated with the melting of antiferromagnetic three-sublattice order when $J_2 = 0.0$, $\Gamma = 0.8$. All other temperature and energy scales are measured in units of J_1 which is set to unity.

consequence of a symmetry-allowed coupling of the form $m_{\text{cl}}|\psi_{\text{cl}}|^3 \cos(3\theta)$ between the static component $m_{\text{cl}}(\vec{r})$ of the uniform magnetization density and the order parameter field ψ_{cl} . In the power-law ordered phase, this coupling is predicted¹⁰ to cause m_{cl} to have the same power-law correlations as $\cos(3\theta)$, leading to a singular χ_u independent of whether the low temperature ordered state is ferrimagnetic or antiferromagnetic. Thus, while the predicted effect is particularly counter-intuitive for the antiferromagnetic case, *i.e.* with $J_2 = 0$ for the system under

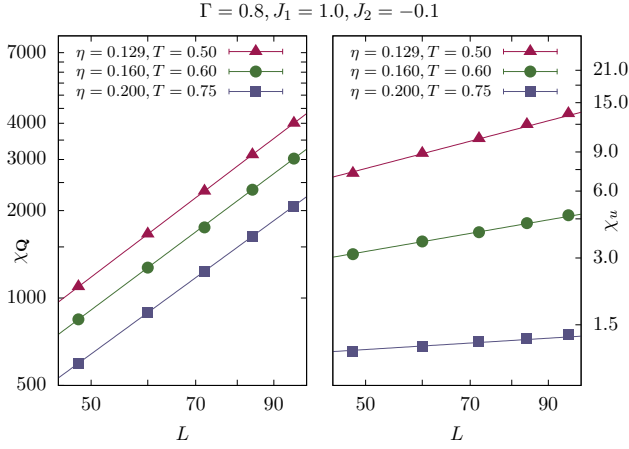


FIG. 8. χ_Q and χ_u fit rather well to power-law forms $k_1 L^{2-\eta}$ and $k_2 L^{2-9\eta}$ respectively for three different values of temperature in the intermediate power-law ordered phase associated with the melting of ferrimagnetic three-sublattice order when $J_2 = -0.1$, $\Gamma = 0.8$. All other temperature and energy scales are measured in units of J_1 which is set to unity.

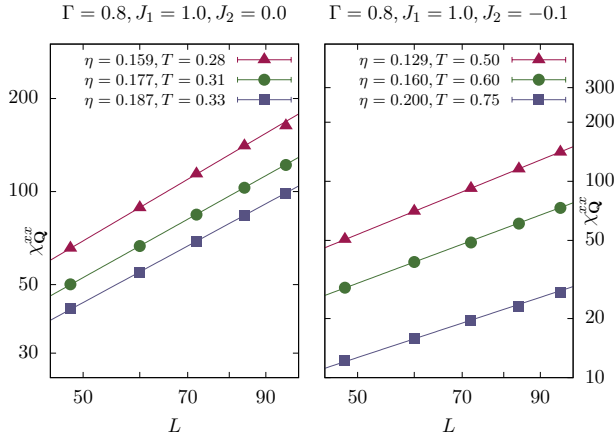


FIG. 9. χ_Q^{xx} fits the power-law form $k_3 L^{2-4\eta}$ for three different values of temperature in the intermediate power-law ordered phase associated with the melting of antiferromagnetic as well as ferrimagnetic three-sublattice order. All other temperature and energy scales are measured in units of J_1 which is set to unity.

consideration, the underlying mechanism is expected to be the same at $J_2 = -0.1$ as well.

As is clear from Fig. 7, simultaneous fits of χ_Q to the form $k_1 L^{2-\eta}$ and χ_u to the form $k_2 L^{2-9\eta}$ work rather well at three different points in the power-law ordered phase associated with the two-step melting of antiferromagnetic three-sublattice order. This can be compared to similar fits in Fig. 8 for the same quantities in the power-law ordered phase associated with the two-step melting of ferrimagnetic three-sublattice order. As is clear from these results, the uniform susceptibility does indeed provide a thermodynamic signature of the power-law ordered

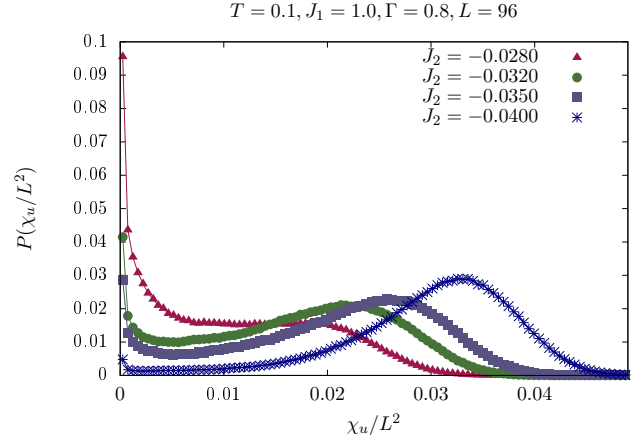


FIG. 10. Histograms of χ_u/L^2 show a characteristic two-peak structure suggestive of a first order transition. All other temperature and energy scales are measured in units of J_1 which is set to unity.

phase, independent of the ferri/antiferromagnetic nature of the low-temperature three-sublattice ordered phase, exactly as predicted by the effective field theoretical arguments of Ref. 10.

A similar argument, which identifies $\beta^{-1} \int_0^\beta \sigma_Q^x(\tau)$ with ψ_{cl}^2 on symmetry grounds, immediately predicts that $\chi_Q^{xx} \sim L^{2-4\eta}$ throughout the power-law ordered phase. As is clear from Fig. 9, our data for χ_Q^{xx} is seen to be completely consistent with this prediction as well.

Finally, we comment on the nature of the transition between the antiferromagnetic and ferrimagnetic three sublattice ordered states. In previous work which studied¹¹ relatively small samples at moderately low temperatures in the vicinity of this transition, the phase of the estimator for the three-sublattice order parameter, as measured in the Quantum Monte Carlo simulations, was seen to be distributed more or less uniformly in the interval $(0, 2\pi)$. If this behaviour were to persist to larger sizes, it would be indicative of a power-law ordered phase that interpolates between the antiferromagnetic and ferrimagnetic three-sublattice ordered phases at nonzero temperature. However, from the Landau theory considerations of Sec. II, we see that the two generic possibilities for this phase transition are first-order behaviour, or an intermediate mixed-phase. An intervening power-law ordered phase can, in this picture, only arise in the fine-tuned limiting case where λ_{12} and higher order anisotropies are all absent. With this in mind, we measure the histogram of the estimator for χ_u/L^2 to look for signals of phase coexistence in the transition region. These histograms are shown in Fig. 10. The two-peak nature of these histograms suggests that the transition is in fact of a weakly first-order type. This is consistent with the fact that the L -dependence of χ_Q is certainly not a power-law, and the fact that Binder ratios of the estimator of χ_Q also do not show a clear crossing (indicative of a second-order

transition),^{24,25} nor do they stick (as they would in a power-law ordered phase).¹⁸ However, we do not see any indications of non-monotonic Binder ratios²⁶ of the type expected in the vicinity of first order transitions. Thus, while our data is suggestive of a weakly first-order transition, more work is needed to clarify the precise nature of this transition.

V. DISCUSSION

Thus, we have obtained fairly convincing evidence for a singular uniform easy-axis susceptibility $\chi_u(B)$ in the power-law ordered phase associated with the two-step melting of antiferromagnetic three-sublattice order in triangular lattice transverse-field Ising antiferromagnets. This (at-first-sight) counter-intuitive thermodynamic signature of two-step melting is already of some general interest, since the transverse-field Ising antiferromagnet on the triangular lattice is a paradigmatic example of the interplay between quantum fluctuations and frustrated classical interactions. Of course, this thermodynamic signature of two-step melting would be of much greater interest and direct experimental relevance if the model Hamiltonian H_{Ising} were to emerge as a good description of magnetic exchange interactions in some frustrated magnet.

In this context, it should be noted that a closely related model Hamiltonian, the one-dimensional transverse field Ising chain, does serve as a good starting point for the theoretical description of an interest-

ing quantum phase transition in the magnetic material Columbite.^{27–29} Columbite can be thought of as a triangular array of one dimensional chains of magnetic moments, with strong intra-chain coupling between the moments and weak inter-chain couplings. This hierarchy of exchange-couplings allows for a theoretical description in terms of the quantum critical properties of the one-dimensional transverse-field Ising chain. It is possible that other materials, with somewhat different exchange pathways but the same strong easy-axis anisotropy, may have much stronger exchange couplings within a triangular plane, and much weaker couplings between planes. For such a material, the model Hamiltonian H_{Ising} could in the same way serve as a good theoretical description, and our results on this thermodynamic signature of two-step melting could then be of direct experimental relevance. We hope that our results provide some motivation for exploring this possibility.

VI. ACKNOWLEDGEMENTS

Our computational work was made possible by the computational resources of the Department of Theoretical Physics of the Tata Institute of Fundamental Research, as well as by computational resources funded by DST (India) grant DST-SR/S2/RJN-25/2006. The analysis of our Monte Carlo data was greatly facilitated by the general-purpose file-handling and data-analysis scripts developed by Geet Rakala.

-
- ¹ J. Villain, R. Bidaux, J. P. Carton, and R. J. Conte, “Critical and multi-critical behavior in a triangular-lattice-gas Ising model: Repulsive nearest-neighbor and attractive next-nearest-neighbor coupling,” *J. Phys. Paris* **41**, 1263–1272 (1980).
 - ² R. Moessner and S. L. Sondhi, “Ising models of quantum frustration,” *Phys. Rev. B* **63**, 224401 (2001).
 - ³ G. H. Wannier, “Antiferromagnetism. The triangular Ising net,” *Phys. Rev.* **79**, 357–364 (1950).
 - ⁴ R. M. F. Houtappel, “Order-disorder in hexagonal lattices,” *Physica* **16**, 425 – 455 (1950).
 - ⁵ J. Stephenson, “Ising model spin correlations on the triangular lattice. III. Isotropic antiferromagnetic lattice,” *Journal of Mathematical Physics* **11**, 413–419 (1970).
 - ⁶ D. P. Landau, “Critical and multi-critical behavior in a triangular-lattice-gas Ising model: Repulsive nearest-neighbor and attractive next-nearest-neighbor coupling,” *Phys. Rev. B* **27**, 5604–5617 (1983).
 - ⁷ S. V. Isakov and R. Moessner, “Interplay of quantum and thermal fluctuations in a frustrated magnet,” *Phys. Rev. B* **68**, 104409 (2003).
 - ⁸ R. Moessner, S. L. Sondhi, and P. Chandra, “Two-dimensional periodic frustrated Ising models in a transverse field,” *Phys. Rev. Lett.* **84**, 4457–4460 (2000).

- ⁹ J. V. José, L. P. Kadanoff, S. Kirkpatrick, and D. R. Nelson, “Renormalization, vortices, and symmetry-breaking perturbations in the two-dimensional planar model,” *Phys. Rev. B* **16**, 1217–1241 (1977).
- ¹⁰ K. Damle, “Melting of three-sublattice order in easy-axis antiferromagnets on triangular and kagome lattices,” *Phys. Rev. Lett.* **115**, 127204 (2015).
- ¹¹ S. Biswas, G. Rakala, and K. Damle, “Quantum cluster algorithm for frustrated Ising models in a transverse field,” *arXiv:1512.00931* (2015).
- ¹² R. G. Melko, “Stochastic series expansion quantum Monte Carlo,” in *Strongly Correlated Systems*, Springer Series in Solid-State Sciences, Vol. 176, edited by A. Avella and F. Mancini (Springer Berlin Heidelberg, 2013) pp. 185–206.
- ¹³ A. W. Sandvik, “Stochastic series expansion method for quantum Ising models with arbitrary interactions,” *Phys. Rev. E* **68**, 056701 (2003).
- ¹⁴ B. Nienhuis, H. J. Hilhorst, and H. W. J. Blote, “Triangular SOS models and cubic-crystal shapes,” *J. Phys. A* **17**, 3559 (1984).
- ¹⁵ E. Domany, M. Schick, J. S. Walker, and R. B. Griffiths, “Classification of continuous order-disorder transitions in adsorbed monolayers,” *Phys. Rev. B* **18**, 2209–2217 (1978).

- ¹⁶ E. Domany and M. Schick, “Classification of continuous order-disorder transitions in adsorbed monolayers. II,” *Phys. Rev. B* **20**, 3828–3836 (1979).
- ¹⁷ S. Alexander, “Lattice gas transition of He on Grafoil. A continuous transition with cubic terms,” *Phys. Lett. A* **54**, 353 – 354 (1975).
- ¹⁸ M. S. S. Challa and D. P. Landau, “Critical behavior of the six-state clock model in two dimensions,” *Phys. Rev. B* **33**, 437–443 (1986).
- ¹⁹ J. L. Cardy, “General discrete planar models in two dimensions: Duality properties and phase diagrams,” *J. Phys. A* **13**, 1507 (1980).
- ²⁰ A. W. Sandvik, “A generalization of Handscomb’s quantum Monte Carlo scheme-application to the 1D Hubbard model,” *Journal of Physics A: Mathematical and General* **25**, 3667 (1992).
- ²¹ O. F. Syljuasen and A. W. Sandvik, “Quantum Monte Carlo with directed loops,” *Phys. Rev. E* **66**, 046701 (2002).
- ²² A. W. Sandvik, “Stochastic series expansion method with operator-loop update,” *Phys. Rev. B* **59**, R14157–R14160 (1999).
- ²³ J. M. Kosterlitz, “The critical properties of the two-dimensional XY model,” *J. Phys. C* **7**, 1046 (1974).
- ²⁴ K. Binder, “Finite size scaling analysis of Ising model block distribution functions,” *Z. Phys. B* **43**, 119–140 (1981).
- ²⁵ K. Binder, “Critical properties from Monte Carlo coarse graining and renormalization,” *Phys. Rev. Lett.* **47**, 693–696 (1981).
- ²⁶ K. Binder and D. P. Landau, “Finite-size scaling at first-order phase transitions,” *Phys. Rev. B* **30**, 1477–1485 (1984).
- ²⁷ A. W. Kinross, M. Fu, T. J. Munsie, H. A. Dabkowska, G. M. Luke, S. Sachdev, and T. Imai, “Evolution of quantum fluctuations near the quantum critical point of the transverse field Ising chain system CoNb_2O_6 ,” *Phys. Rev. X* **4**, 031008 (2014).
- ²⁸ S. Lee, R. K. Kaul, and L. Balents, “Interplay of quantum criticality and geometric frustration in Columbite,” *Nature Physics* **6**, 702–706 (2010).
- ²⁹ R. Coldea, D. A. Tennant, E. M. Wheeler, E. Wawrzynska, D. Prabhakaran, M. Telling, K. Habicht, P. Smeibidl, and K. Kiefer, “Quantum criticality in an Ising chain: Experimental evidence for emergent E8 symmetry,” *Science* **327**, 177–180 (2010).